Laser Manufacturing: Strategies for dealing with the challenges

John R. M. Barr*,
SELEX Galileo Ltd, 2 Crewe Toll North, Edinburgh, EH5 2XS, UK.

ABSTRACT

Laser manufacturing in Edinburgh was initiated in 1963 by Ferranti (one of the previous names for SELEX Galileo). Since 2003 a modernized range of military lasers has been established. Innovation, both technical and in other aspects of the business, has enabled the design and manufacture of world leading laser designators and countermeasure lasers. Specific examples will be given including: the application of Geometric Algebra to resonator design; novel alignment free optical parametric oscillators; techniques for designing thermally insensitive laser diode pump heads; and methods for contamination control in lasers.

Keywords: Optical parametric oscillator, ring resonators, Geometric Algebra, laser designators,

1. INTRODUCTION

Creating facilities for manufacturing lasers in volume requires good design capabilities, excellent execution and a robust and reliable supply chain. Many companies have achieved this goal; this is how SELEX Galileo has tackled the challenge during the last 8 years. The starting point was not a clean sheet of paper, but an organization that had successfully manufactured lasers throughout the 1970's and 1980's into the early 1990's. There was a long gap until 2005, when the next Edinburgh designed laser entered production. This paper gives an overview of the early company history in laser manufacturing as background for our own 50th anniversary of laser design and production in 2013. Several recent technical innovations are then reviewed: high energy laser resonators in Section 2; thermally insensitive lasers in Section 3; some comments on reliability of lasers in Section 4; and the paper closes with some other aspects of laser design that experience suggests can be important in Section 5.

1.1 Background

The story starts in 1963 when the Valve Department in Edinburgh, led by Neil Forbes and Graham Clarke, introduced the Ferranti Gas Laser Mk 1[1] into commercial production. This device was a HeNe laser and was used primarily for research by Universities within the UK. The background in gas lasers ultimately led to the development of CO_2 lasers for machining produced out of the Ferranti facility in Dundee. Over 500 MF400's were built starting in the early 1970's[2]. CO_2 laser manufacturing in Dundee continued under a variety of company names (Laser Ecosse, from 1990; Howden Laser from 1995; and finally Ferranti Photonics from 2000 until 2005). The success of this product line was based on the small footprint of the MF400 allowing unanticipated flexibility by mounting the laser directly on the moving cutting head.

The next stage of the story emerges in the late 1966 when a separate group within Ferranti in Edinburgh, including Muir Ainslie, won a contract to develop an electro-optic air to ground targeting system for UK aircraft such as the Jaguar, Harrier and Tornado[3]. The system contained a low divergence rangefinder and a laser spot tracker in a stabilized head mounted within the aircraft nose cone. Initially the laser was based on a Westinghouse design, obtained though a technology exchange agreement – Edinburgh radar technology in exchange for a laser design. As the transition to a production variant of the Laser Rangefinder and Marked Target Seeker (LRMTS) was considered in 1969, it was recognized that the Westinghouse design was not suited for application in severe environmental conditions. The resonator, a single Porro prism with a plane output coupler, was not perturbation stable. An alternate design was required: a crossed Porro design, which is perturbation stable, combined with polarization controlled Q-switching was developed[4]. This new design transitioned into production and approximately 900 units were produced, some of which are still in service today. The crossed Porro resonator developed for the LRMTS was scaled in output energy and used to develop a man portable laser designator, the Type 306, starting in 1972. This system was first used during the Falklands conflict in 1982.

* john.barr2@selexgalileo.com ; Phone +44 (0)1313434043; www.selexgalileo.com

In 1980 the development of a targeting system known as the Thermal Imaging and Laser Designation pod (or TIALD pod) was initiated which contained the Type 126 laser designator. It was during this period that performance issues were noted with Lithium Niobate Q-switches. The pyroelectric effect results in charge build up, particularly at low temperature, which reduces the contrast ration of the Q-switch resulting in laser unwanted break-through or pre-lase. The solution developed in Edinburgh[5] uses a radioactive source of alpha particles to increase air conductivity and dissipate the pyroelectric charge, thus preventing pre-lase. It is worth noting that this solution is widely adopted, but the customer preference for a non-radioactive based solution has driven the development of alternative approaches.

A further development in 1990 was the application of HeNe lasers to ring laser gyros. These have found a niche market as a key component of artillery pointing systems and are still in production today. Images of some of the early lasers and systems are shown in Figure 1.
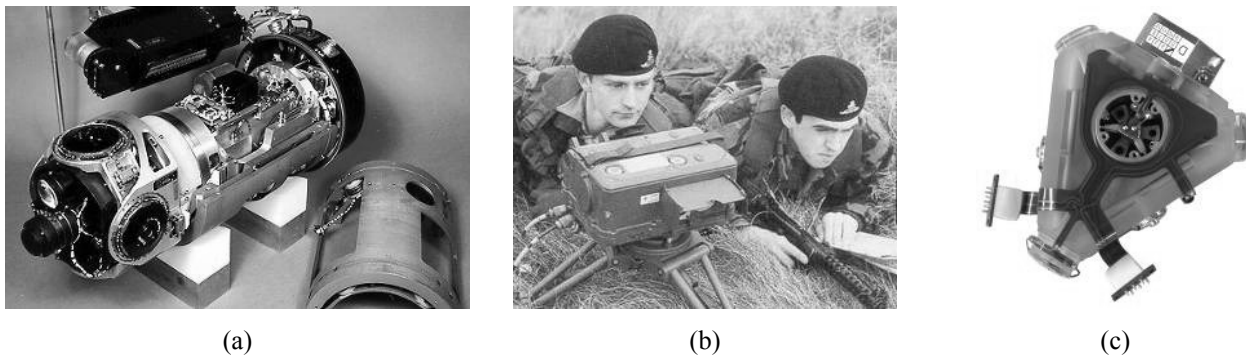

| (a) | (b) | (c) |

Figure 1. Early laser products: (a) a Laser Rangefinder and Marked Target Seeker, and (b) Type 306 man portable laser designator, and (c) a ring laser component of a gyro.

The reintroduction of solid state laser manufacturing in 2005 was the direct result of winning a contract to build the laser designator for the F-35 Joint Strike Fighter. During the late 1990's, continuing investment in laser technology ensured that laser design and skills were maintained. New technology was continually assessed and ways of exploiting its potential meant that new pump sources (laser diodes arrays), new devices (optical parametric oscillators) and new wavelength regions (for countermeasures) were available for use. It is fair to say the pace of change accelerated since 2005 under impetus and challenge of a revitalized manufacturing environment and the newer laser designs differ radically from their predecessors. The trend is to smaller lasers (improved packages), more reliable lasers (continual feedback from users), more efficient lasers (introduction of temperature insensitive pump heads), lightweight lasers (new materials), and lasers that are cheaper to own and operate (attention to cost of materials and manufacturing processes). New functions have been introduced such as variable divergence to aid the use of active illumination where the laser illuminates a target and the scattered light is used to form an image.

2. HIGH ENERGY LASER RESONATORS

In this part of the paper, the topic of Q-switched lasers with output energy in the 50 to 350mJ and pulse durations around 15ns will be discussed. These resonators have to meet the conflicting requirements of avoiding laser damage, which requires large mode areas, and having reasonable beam quality ($2<M^2<8$), which drives small mode areas. Furthermore, the resonator must be insensitive to perturbations arising from thermal or vibrational effects. Obvious solutions to this problem may be found in the ubiquitous crossed Porro resonator [5, 6, 7] and also in unstable resonators[8]. A similar problem arises in the design and packaging of Optical Parametric Oscillators where lasers with the high energy lasers are used as pump sources.

The approach taken by SELEX Galileo has been to reanalyze the basic resonator properties and to identify different approaches which offer packaging advantages. To this end a mixture of techniques are used, ranging from ray tracing to a novel application of Geometric Algebra[9, 10] to laser resonators.

Geometric Algebra provides an alternate technique to analyze and understand optical systems, which presents many advantages compared with standard vector and matrix toolsets once the new mathematical techniques are understood. A very much abbreviated discussion is presented here in order to provide an overview and demonstrate the benefits this approach provides.

2.1 Introduction to Ray Tracing Using Geometric Algebra

Geometric Algebra (GA) combines the traditional inner ($\mathbf{a} \cdot \mathbf{b}$) and outer product ($\mathbf{a} \times \mathbf{b}$) of vectors into a geometric product, defined between two vectors, $\mathbf{a}$ and $\mathbf{b}$ as:

$$\mathbf{ab} = \mathbf{a} \cdot \mathbf{b} + \mathbf{a} \wedge \mathbf{b} = \mathbf{a} \cdot \mathbf{b} + \mathbf{i}\mathbf{a} \times \mathbf{b}$$

where $\mathbf{i}$ is the pseudo-scalar for 3D space. Note that both scalars and pseudo-scalars commute with all members of the 3D algebra. The 3D algebra contains four fundamental quantities: scalars, vectors, bivectors (for example $\mathbf{a} \wedge \mathbf{b} = \mathbf{i}\mathbf{a} \times \mathbf{b}$) and pseudo-scalars. A general multi-vector is the sum of one or more examples of each of these quantities.

Reversing the order of the vectors in the GA product produces

$$\mathbf{ba} = \mathbf{a} \cdot \mathbf{b} - \mathbf{i}\mathbf{a} \times \mathbf{b}$$

whence it is possible to show that parallel vectors commute ($\mathbf{ab} = \mathbf{ba}$) and perpendicular vectors anti-commute ($\mathbf{ab} = -\mathbf{ba}$). In general the geometric product of two vectors is the sum of a scalar and a bivector while the product of three vectors is the sum of a vector and a pseudo-scalar. Similarly, the product of an even number of vectors is also the sum of a scalar and a bivector while the product of an odd number of vectors is the sum of a vector and pseudo-scalar. This property of the 3D GA turns out to be the basis of the well known result that a true optical image rotation is achieved with an even number of reflections.

Finally it is easy to show that expressions for the inner product and the outer product in terms of the geometric product are $2\mathbf{a} \cdot \mathbf{b} = \mathbf{ab} + \mathbf{ba}$ and $2\mathbf{i}\mathbf{a} \times \mathbf{b} = \mathbf{ab} - \mathbf{ba}$.

The law of reflection of an incident ray $\mathbf{v_1}$ from a plane mirror with normal $\mathbf{n_1}$ can be derived in GA to be:

$$\mathbf{v_2} = -\mathbf{n_1}\mathbf{v_1}\mathbf{n_1} = -\mathbf{n_1}(2\mathbf{n_1} \cdot \mathbf{v_1} - \mathbf{n_1}\mathbf{v_1}) = \mathbf{v_1} - 2(\mathbf{n_1} \cdot \mathbf{v_1})\mathbf{v_1}$$

where the equivalence with the standard vector notation for reflection of rays from mirrors[11] is explicitly demonstrated (all vectors have unit magnitude).

The output ray, $\mathbf{v_m}$, from a sequence of m plane mirrors is therefore easily found to be:

$$\mathbf{v}_m = (-1)^m \mathbf{n_m}\mathbf{n_{m-1}}..\mathbf{n_1}\mathbf{v_1}\mathbf{n_1}..\mathbf{n_{m-1}}\mathbf{n_m} = (-1)^m \mathbf{U}^*\mathbf{v_1}\mathbf{U}.$$

where $\mathbf{U} = \mathbf{n_1}..\mathbf{n_{m-1}}\mathbf{n_m}$ and $\mathbf{U}^* = \mathbf{n_m}\mathbf{n_{m-1}}..\mathbf{n_1}$. The property $\mathbf{U}^*\mathbf{U} = 1$ is easily demonstrated. This equation may be applied to optical resonator analysis by requiring that after one round trip the output ray is equal to the input ray: $\mathbf{v_m} = \mathbf{v_1}$; hence $\mathbf{U}\mathbf{v_1} = (-1)^m \mathbf{v_1}\mathbf{U}$. The ray, if it exists, is known as the optic axis. If m is even, then $\mathbf{v_1}$ and $\mathbf{U}$ commute; otherwise for m odd, $\mathbf{v_1}$ and $\mathbf{U}$ anti-commute.

The following important result will now be quoted; the proof may be found in the references[9, 10]. The form of U for an even number of mirrors is $\mathbf{U} = \cos(\alpha) + \mathbf{i}\boldsymbol{\sigma}\sin(\alpha)$ (as noted earlier, a scalar plus a bivector). When applied to a vector $\mathbf{y}$ in the form $\mathbf{U}^*\mathbf{y}\mathbf{U}$ the output is the rotation of $\mathbf{y}$ around $\boldsymbol{\sigma}$ in a right-handed sense through an angle 2α. If U represents a laser resonator with an even number of mirrors, then $\mathbf{v_1}$ and $\mathbf{U}$ commute as stated earlier. Further, since $\mathbf{v_1}$ commutes both with the scalar part and with the pseudo-scalar $\mathbf{i}$ it must be concluded that $\mathbf{v_1}$ and $\boldsymbol{\sigma}$ must also commute. Hence $\mathbf{v_1} = \boldsymbol{\sigma}$, $\mathbf{U} = \cos(\alpha) + \mathbf{i}\mathbf{v_1}\sin(\alpha)$ and we come to the remarkable conclusion that U allows the direction of the optic axis to be deduced for a resonator containing an even number of mirrors. Furthermore, if we let $\mathbf{w}$ represent a vector perpendicular to $\mathbf{v_1}$, such that $\mathbf{w}$ can represent points on a beam centered on the optic axis, we find that $\mathbf{U}^*\mathbf{w}\mathbf{U}$ represents a rotation in a right-handed sense around $\mathbf{v_1}$ through an angle 2α and conclude that U also contains information regarding the image rotation for a single pass around the resonator.

Some familiar examples may help to demonstrate the power of this approach. Consider the important problem of stability of a ray direction when optical components through which it transits are rotated. Denote the rotation of the components by $R = a + i\sigma b$ (the form of rotations is always the same in GA, compare with the expression for U). The transmitted ray through the rotated optical system is:

$$\mathbf{v}_m = R^* U^* R \mathbf{v}_1 R^* U R$$

If R commutes with U then the transmitted ray, $\mathbf{v}_m$, does not change. However, R only commutes with U if U is either a scalar or a pseudo-scalar. For example, a two mirror sequence meets this requirement only if $U_2 = \mathbf{n}_1 \mathbf{n}_2 = \mathbf{n}_1 \cdot \mathbf{n}_2 + i\mathbf{n}_1 \times \mathbf{n}_2 = 1$ which is true when $\mathbf{n}_1 = \mathbf{n}_2$. This is, of course, a periscope. Likewise, it is straightforward to show that the three mirror case, $U_3 = \mathbf{i}$, requires that the three mirror normals are mutually perpendicular. This is, of course, a corner cube. The conclusion is that there is one example of a two mirror device that is perturbation stable (the periscope) and one example of a three mirror device that is also perturbation stable. There are also a group of two mirror sequences that exhibit partial stability. The general form for U_2 is $U_2 = \cos(\alpha) + i\sigma \sin(\alpha)$. Attempting to rotate U_2 around σ leaves U_2 unchanged; hence the output ray from this sequence of mirrors is not perturbed by the physical rotation around σ. Again this is a familiar result, but derived in a very economical fashion. These conclusions are in agreement with those found in the context of matrix representations for mirrors[12].

The final results quoted here relate to the detailed ray trace around a resonator composed of an even number of mirrors. For illustration purposes only, this will be taken to have four mirrors. The optic axis $\mathbf{v}_1$ may be calculated using $U = \mathbf{n}_1 \mathbf{n}_2 \mathbf{n}_3 \mathbf{n}_4$ as discussed earlier. Take the ray striking the first mirror (with normal $\mathbf{n}_1$) as $\mathbf{v}_1$. It is then reflected: $\mathbf{v}_2 = -\mathbf{n}_1 \mathbf{v}_1 \mathbf{n}_1$ and propagates a length $L_2 \mathbf{v}_2$ to the second mirror (with normal $\mathbf{n}_2$) and so on. The fourth and final ray $\mathbf{v}_4$ returns to the fourth mirror (with normal $\mathbf{n}_4$) and is reflected into $\mathbf{v}_1$. This process defines the position and orientation of each of the four mirrors.

Next, consider the impact on the resonator by varying the angle of one mirror, $\mathbf{n}_4$ say, by a small angle η around a vector σ lying in the mirror plan (i.e. normal to $\mathbf{n}_4$). The new normal is $\mathbf{n}_4' = R^* \mathbf{n}_4 R = \mathbf{n}_4 R^2$ because σ and $\mathbf{n}_4$ anti-commute since they are defined to be mutually perpendicular. Hence U becomes $U' = \left(a' + b' i \mathbf{v}_1\right) = \mathbf{n}_1 \mathbf{n}_2 \mathbf{n}_3 \mathbf{n}_4 R^2 = \left(a + b i \mathbf{v}_1\right) R^2$. In the limits of small (paraxial) rotations then an approximation for R may be found as $R = \cos\left(\frac{\eta}{2}\right) + \sin\left(\frac{\eta}{2}\right) i\sigma \approx 1 + \frac{\eta}{2} i\sigma$. Solving for $\mathbf{v}_1'$ yields

$$\mathbf{v}_1' = \mathbf{v}_1 + \eta\left(-\frac{a}{b}\sigma \cdot \mathbf{v}_1 \mathbf{v}_1 + \frac{a}{b}\sigma + \sigma \times \mathbf{v}_1\right) = \mathbf{v}_1 + \eta\delta_1$$

where δ_1 can be shown to be a vector perpendicular to $\mathbf{v}_1$ (but it is not a unit vector – its magnitude depends on a and b). Provided this equation has a valid solution (i.e. $b \neq 0$ or U is not purely scalar) then the ray direction is changed by a small, but finite amount. In addition to the change in angle, there is also a displacement relative to the unperturbed optic axis location. A vector representing the altitude of the ray relative to the unperturbed position is $\mathbf{y}_1$ at the start of leg 1 and $\mathbf{y}_1' = \mathbf{y}_1 + \eta L_1 \delta_1$ at the end of leg 1. Propagating this around the resonator results in the following expression:

$$\mathbf{y}_1 = \frac{\left(\left(U^*\right)^2 - 1\right)}{2 - \left(U^2 + \left(U^*\right)^2\right)} \eta L \delta_1$$

where $L = \sum_{i=1}^{4} L_i$.

The important conclusion resulting from this is that the ray path is well defined in angle and position providing that $b \neq 0$ or equivalently, U is not purely scalar.

This analysis demonstrates that the beneficial features of a crossed Porro resonator are shared by many plane multi-mirror resonators designs providing that:

(a) An even number of plane mirrors are used for each round trip; and

(b) The image rotation angle is >0 and not a multiple of 360°. If constructed as a ring resonator, then this must be a non-planar ring.

(c) While it has not been demonstrated here, the similarity between the crossed Porro resonator and the non planar ring resonator is straightforward to show. Consider a 4 mirror non-planar ring resonator with perimeter lengths L_1, L_2, L_3 and L_4. This may be transformed into the crossed Porro resonator by setting $L_1=L_3=0$; $L_2=L_4$; and $\mathbf{n_1} \cdot \mathbf{n_2} = \mathbf{n_3} \cdot \mathbf{n_4} = 0$. Thus the crossed Porro resonator may be regarded as a special case of a non-planar ring resonator.

2.2 Application to high energy resonator design

The previous analysis shows that the beneficial features possessed by a crossed Porro resonator can be replicated in other arrangements with different and useful properties. The specific example discussed here is a non planar ring resonator for an Optical Parametric Oscillator (OPO). This project started as a feasibility demonstration where the objective was to design an OPO, suitable for use in close proximity with a high energy pump laser, and target output energy of the order of 100mJ per pulse. A ring laser was selected as the preferred resonator type because the geometry minimizes back reflections into the high energy pump laser. The initial design is shown in Figure 2, together with some beam profiles. Note that this is a planar ring, for which U=1, there is no pattern rotation and the system does not possess an optic axis. The beam shape distortion over temperature is characteristic of a resonator that is not perturbation stable.
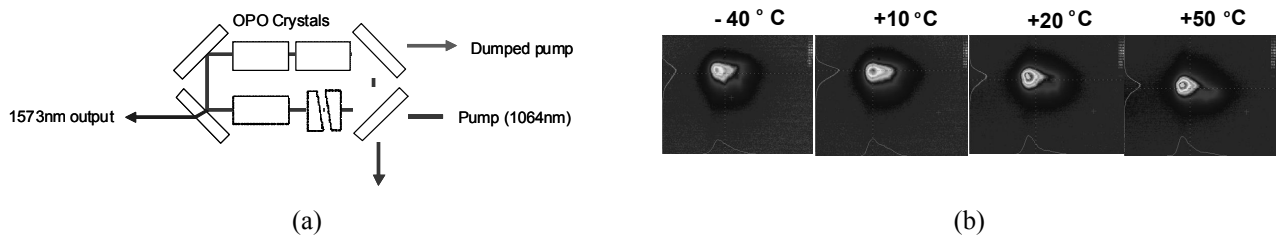

Figure 2. (a) Initial OPO configuration and (b) beam shape variation over temperature.

The motivation to look at non-planar ring resonators came from a paper on the monolithic non-planar ring oscillator[13] and a later paper on non-planar rings applied to parametric oscillators[14]. The key observation[13] is that the non-planar ring is perturbation stable: it always possesses an optic axis. The development of the GA analysis summarized in section 2.1 provides a clear understanding of why non-planar rings were special and to help understand how crossed Porro resonators fitted in to the picture.

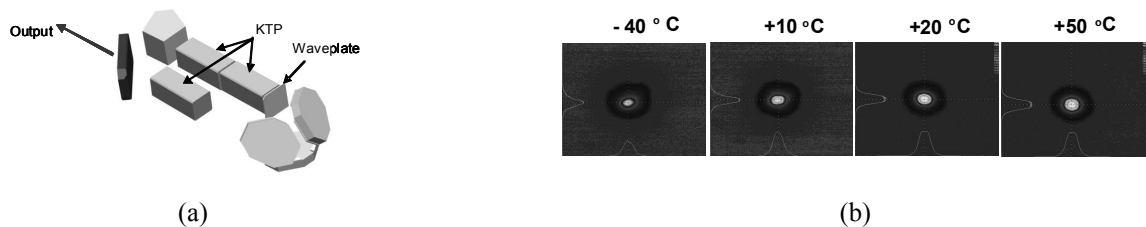The solution adopted by SELEX Galileo is shown in Figure 3.

Figure 3. (a) Final 6 mirror non-planar ring OPO configuration (the output mirror is labeled 1 and the ring is traversed in a clockwise direction) and (b) the improved beam shape variation over temperature.

A six mirror OPO was selected because this allowed a very simple planar package, more compatible with the system than alternate four mirror designs[14]. The image rotation is provided by the three mirror non planar sequence at the right hand end of Figure 3(a). These could have been manufactured from a prism, looking very much like a modified corner cube; however it was necessary to introduce the pump beam through one of these reflecting surfaces so a solution

composed of three identical mirrors was selected. The penta prism was chosen as a space effective way to ensure an even number of reflections on each round trip.

90° image rotation on each round trip was selected to improve the symmetry and uniformity of the laser output. A point on the OPO signal samples 4 spatially independent parts of the pump beam which allows for a measure of spatial averaging. From a laser manufacturing perspective the adoption of a true perturbation design allowed the implementation of an alignment free OPO. The six mirrors shown in Figure 3 are bonded to an aluminum chassis with no precision active alignment required. The benefit is a more reliable product with reduced touch time compared to a non perturbation free design.

The details of the design may be found elsewhere[15]. The mirror normals and the calculated round trip parameters are provided as examples in Figure 4. As noted earlier the general form of U_6 (since it contains an even number of mirrors) is $U_6 = \cos(\alpha) + \mathbf{i\sigma}\sin(\alpha) = \cos(135°) + \mathbf{i}(-\mathbf{x})\sin(135°)$ The bi-vector part of U_6 (i.e. $-\mathbf{ix}$) shows the optical axis immediately prior to the output coupler (mirror 1) is $-\mathbf{x}$ (the axis system is defined in Figure 4). The image rotation angle may be deduced from U_6 to be $2\alpha = 270°$ in a right handed sense around $-\mathbf{x}$ or 90° in a left handed sense around $-\mathbf{x}$.

$$\mathbf{n_1} = \tfrac{1}{\sqrt{2}}(\mathbf{x} + \mathbf{y}) \qquad \mathbf{n_2} = \tfrac{1}{\sqrt{2(2+\sqrt{2})}}\left(\mathbf{x} + \left(1 + \sqrt{2}\right)\mathbf{y}\right) \qquad U_p = \mathbf{n_2}\mathbf{n_3} = \tfrac{1}{\sqrt{2}}(-1 + \mathbf{i}z)$$

$$\mathbf{n_3} = \tfrac{1}{\sqrt{2(2+\sqrt{2})}}\left(\left(1 + \sqrt{2}\right)\mathbf{x} + \mathbf{y}\right) \qquad \mathbf{n_4} = \tfrac{-1}{2}\left(\sqrt{2}\mathbf{x} + \mathbf{y} + \mathbf{z}\right) \qquad U_R = -\mathbf{n_3}\mathbf{n_4}\mathbf{n_5} = \tfrac{1}{\sqrt{2}}(\mathbf{x} + \mathbf{i})$$

$$\mathbf{n_5} = \mathbf{z} \qquad \mathbf{n_6} = \tfrac{-1}{2}\left(\sqrt{2}\mathbf{x} - \mathbf{y} + \mathbf{z}\right) \qquad U_6 = \mathbf{n_1}U_pU_R = \tfrac{1}{\sqrt{2}}\left(-1 + \mathbf{i}(-\mathbf{x})\right)$$

(a) (b)

Figure 4. (a) OPO mirror normals. (b) Calculations of U for the resonator (made up from U_p for the penta prism and U_R for the 3 mirror image rotator). The axis directions are defined as follows: $\mathbf{x}$ points from the output coupler towards the rear three mirror assembly; $\mathbf{y}$ points from the output coupler towards the penta prism; and $\mathbf{z}$ completes a right handed system by pointing vertically out of the OPO plane.

The benefits of the non-planar ring geometry applies not only to the OPO, but has been used to improve the performance of Nd:YAG lasers as well.

3. THERMALLY INSENSITIVE LASER DESIGNS

The use of semiconductor laser diodes traditionally requires temperature stabilization of the diodes in order to maintain their output wavelength at the optimal value for good absorption. Typically for man portable applications reduced power consumption is beneficial and rapid switch on times are essential. Two strategies are used to mitigate the loss in pump absorption and minimize the variation in output energy over temperature: (a) fix the laser wavelength perhaps by using a Volume Bragg Grating[16] (VBG) or other technique, and (b) accept some variability in wavelength and engineer the absorption side to minimize the impact of wavelength variation from the pump (perhaps by increasing the doping level or through increasing the absorption path length). Directions of development for both these objectives will be discussed. The generic constraint put on the project is that the solution should maximize commonality with existing laser designs, should not increase the product cost, but should indeed reduce it (see section 5(d)). It was therefore decided that the solution shall work with a side-pumped geometry and shall utilize un-collimated laser diode stacks. The Nd:YAG gain material is a 5mm square cross section zigzag slab. The base of the slab is coated to provide a high reflection around 808nm. Throughout this section the laser diodes used in the experiments were provided by Lasertel Inc.

3.1 Thermally Insensitive Laser Diode Arrays using Volume Bragg Gratings

The use of VBGs in conjunction with quasi-CW stacks has been examined in order to verify if they had utility in reducing the sensitivity of wavelength to temperature change. Two different build standards of laser diode were used in the assessment which concluded with the demonstration of a Nd:YAG laser over an extended, but not the complete, military temperature range.
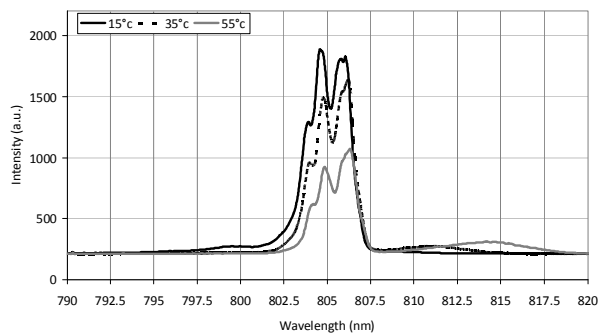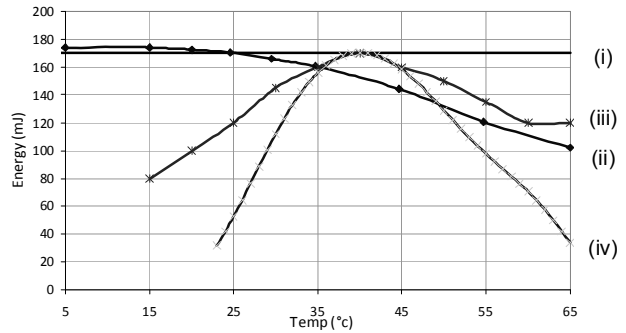
Figure 5. (a) Variation in the VBG stabilized laser diode array wavelength over temperature, (b) Each trace is labeled as follows: (i) Measured thermally controlled laser diode pumped Nd:YAG output; (ii) Measured VBG stabilized laser diode pumped Nd:YAG laser output; (iii) Measured laser diode pumped Nd:YAG output with no temperature stabilization of the laser diodes; and (iv) Calculated variation in output energy from a laser diode pumped Nd:YAG laser over temperature.

It is clear from the data shown in Figure 5 that the VBG stabilized laser diode arrays significantly reduce the variation in output energy over temperature, but not to the full range that the application requires. Following this work, continued development has taken place using new VBG materials and different laser diode designs in order to further improve performance.

3.2 Increasing the absorption path length

This work described in the previous section (section 3.1) does show an interesting feature worth further consideration. The calculated output energy curve using non-thermally stabilized laser diode arrays (Figure 5(b)(iv)) does not agree with the measured curve (Figure 5(b)(iii)). In fact the measured energy curve is markedly more relaxed: the laser produces more energy over a wider temperature range than predicted. The reason is not obvious and in fact has been observed many times and put down to as an interesting feature and a welcome relaxation in the temperature stabilization requirements.

Recently the cause of the difference between the two curves has been identified. It is caused by multiple reflections from the laser diode array, in particular from the spacers in the laser diode array, allowing the non absorbed pump light to make additional passes through the gain material. The calculated curve in Figure 5(b)(iv) assumes a double path absorption length of 10mm and ignores the multiple reflections. The absorption length characteristic of the measured data shown in Figure 5(b)(iii) is estimated to be approximately 17mm and is caused by multiple reflections between the laser diode array and the base of the zigzag slab.

Once this is understood, there are several ways in which the effect can be enhanced to provide an increased absorption path length. Two particularly effective modifications to the laser diode arrays have been identified and tested:

(a) Our original configuration contained 10 bar stacks orientated so that the fast axis divergence was across the width of the Nd:YAG zigzag slab. Each bar is 10mm long and spaced at 400μm. Similar peak power devices can now be obtained with 5mm long emission regions so it is possible to re-orientate the bar so the fast axis divergence is now orientated along the length of the slab.

(b) The spacer size can be increased from 400μm up to several mm in length which increases the overall reflection surface within each laser diode array.

By these means it has been possible to increase the effective absorption length to approximately 35mm in a 5mm deep slab. Figure 6 shows the effective absorption of the pump over a wide temperature range for three different effective absorption lengths.
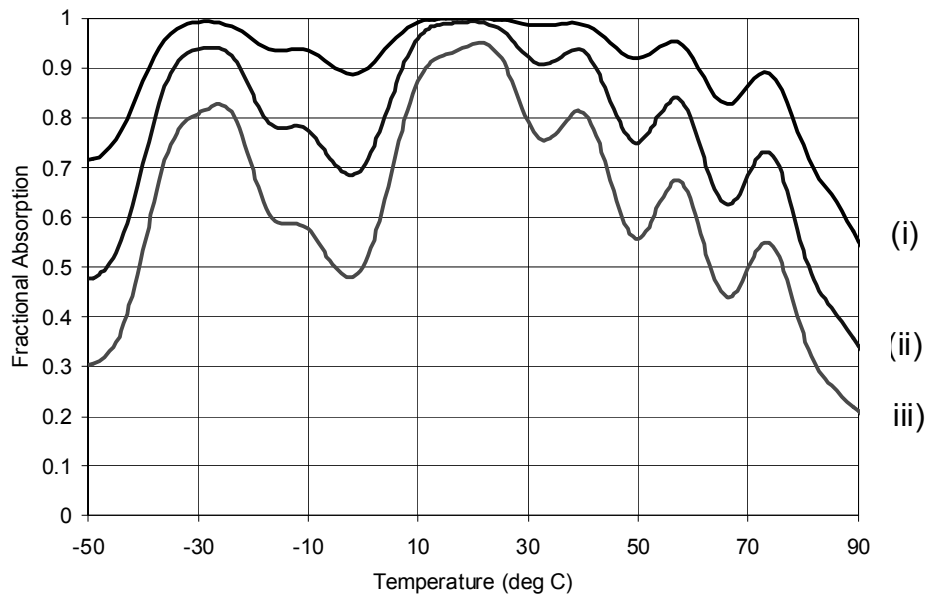
Figure 6. Calculated absorption of pump light with a 2.5nm line width for three different effective absorption lengths: (i) 36mm; (ii) 17mm and (iii) 10mm.

It is clear that these relatively straightforward modifications to the laser diode array geometry promotes an increased absorption and substantially reduces the sensitivity of the level of absorption to temperature change. This observation clearly has utility in addressing the design of thermally insensitive lasers. This approach has also been used to side pump relatively thin slabs (square cross-section, 3mm length) such that the standard absorption fraction is small. The use of this simple and innovative solution increases the absorption length and allows an efficient side pumped laser to be realized.

Excellent thermal insensitivity can be obtained through the use of a relatively narrow line width pump source. It is unnecessary to make use of the multi wavelength diodes to achieve temperature insensitive operation.

4. RELIABILITY OF LASERS

Lasers are widely believed to be unreliable by military users. Fortunately things are changing and the introduction of new technologies has improved laser reliability significantly. The new technologies include: the introduction of lasers diodes as pump sources; the introduction of conduction cooling from heat sources to the heat sink and the consequential avoidance of liquid filled optical heads; new adhesives and other fixing techniques; modern electronics; general improvements in materials and coatings. The achievement of high reliability in a newly designed product means that the well known bath tub curve has to be transited as rapidly as possible. One tool to enable this is attention to Root Cause and Corrective Action as discussed in Section 5(c).

Once through the early stages of the bath tub and the removal of early life failure modes, various long term wear out mechanisms become important. Apart from known and well understood mechanisms (for example the life of laser diode arrays), the ultimate failure mode of high energy density lasers arises when an optics degrades or optical damage occurs, resulting in an energy drop[18, 19, 20]. Laser damage is particularly important in sealed units such as those required for rugged environments, because there is a long term build up of gas species due to out gassing from adhesives, seals, wiring harnesses and other components within the optical module. The long term degradation mode appears to be a photo deposition process where layers of absorbing material are deposited on optics from the gaseous material contained within the optical module and probably enhanced by being adsorbed onto the optic surface[18]. The challenge faced by laser designers is to understand how to maximize the laser lifetime and coping with these wear out mechanisms while still designing affordable and manufacturable lasers. It is fair to say the understanding of contamination mechanisms is not complete and an element of judgment is required.

The approach to this problem taken by SELEX Galileo is, by necessity, multi level. It is not sufficient to select allowable materials, but controls must also be put in place to ensure that the handling and supply of parts is clean that contamination is not inadvertently added to a component.

(a) The starting point is to ensure that the Laser Damage Threshold (LDT) of all optics exceeds the worst case energy density by a sufficient margin (see section 5(a)). The supplier of each optic is engaged and a process agreed where the LDT is verified regularly, either on a batch basis or other acceptable rate.

(b) The handling and assembly process is defined in order that the optic LDT is not compromised through within SELEX Galileo. A local LDT measurement company[21] is used to verify that the LDT of components remains unchanged through this activity. New processes are benchmarked in this fashion.

(c) The material selection is limited to a controlled palate of materials in order to minimize the potential for damage. These materials have been shown not to promote long term LDT degradation either from experience in other lasers or through specific test regimes[18, 19, 20].

(d) There is evidence, both based on our own observations and from elsewhere[22], that Ion Beam Sputtered (IBS) coatings are less prone to suffer a reduction in LDT over time compared to e-beam coatings. This feature is attributed to the higher density achieved in IBS thin film coatings which may reduce the level of gaseous species absorbed onto the coating surface.

(e) Unfortunately, our experience suggests that the supporting information is seldom clear and not always available in a timely or cost effective fashion. We therefore also rely on generic risk mitigation processes which include: ensuring that the atmosphere within the laser is always a N_2/O_2 mix since the presence of O_2 is well known to reduce the build up of absorbing layers on optics[23]; and routinely vacuum out gassing and cleaning assemblies and other components[20].

The combination of these processes provides assurance that the design and build processes produce laser systems capable of operating reliably for long periods of time. SELEX Galileo has observed 10x reliability increase moving from flashlamp pumped systems to modern designs.

5. PROCESS IMPROVEMENTS

Designing and manufacturing lasers within a generalized engineering organization presents a number of benefits and, inevitably, some challenges. One of the strengths of a larger organization is the focus on process and continuous improvement. This is particularly beneficial in developing and implementing good practice since there is continual feedback and support. The main challenge arises from the lack of product domain knowledge of all individuals within the larger organization.

Specific examples of the types of improvements to design practice that have been developed and embedded within the organization will now be discussed.

(a) **Design and Manufacturing Margin control.** The standard engineering design process focuses on meeting key customer requirements. Within SELEX Galileo, the normal practice is to ensure that the design has sufficient margin so that it is capable of being manufactured easily. The product must be capable of meeting its requirements when various insets such as environmental effects, life degradation, measurement uncertainty and finally an estimate of the manufacturing distribution for the parameter is taken into account. The analysis may be based on predictions or hard data from suppliers and from the shop floor.

(b) **Sightline control.** One key requirement for lasers is the confidence that the laser beam is pointing where intended. Environmental perturbations such as vibration and temperature variation cause the laser chassis to distort and potential impact the laser sightline. It is important that this requirement is addressed at the design stage where there is flexibility to manage the thermal gradients of the structure over temperature. A sightline modeling technique has been developed and proven through a number of laser designs. Finite element analysis is used to predict thermal profiles and then to calculate the structural deformations. The subsequent movement of the optical components results in changes in sightline. A similar tool chain is used to predict sightline movement when vibration is taken into account.

(c) **Root Cause and Corrective action (RC&CA).** It seems strange to talk about an activity that should be core to a business and certainly underpins certification to ISO9001/9100 and other quality standards. However, experience suggests that it is a topic that often only recieves full attention of a business when a customer raises an issue. The benefits of taking RC&CA seriously are many: rapid correction of defects reducing the cost of failure internally and for the customer; improvements in product reliability; reduction in variation and a more consistent production flow. An empirical benefit of change, resulting from fault resolution, is a reduction in cost. Engineers tend to find it easier to reduce the cost of an existing assembly, than controlling cost during a white paper design process. RC&CA has been emphasised within the organization by establishing a preferred approach, based on a simplified DMAIC (Define/Measure/Analyse/Improve/Control) process. However, simple provision of a tool will not work without a senior oversight and involvement; a regular (every two weeks) sector review is held which monitors progress on key RC&CA issues and provides feedback, support and knowledge sharing. Attention to RC&CA is recognized as being instrumental in rapidly driving out the early life cycle "infant mortality" associated with introducing new laser technology and achieving the predicted 10x reliability improvements offered by new technology (for example transitioning from flashlamps to laser diodes).

(d) **Cost control.** Everyone in an engineering organization will recognize the importance of cost and cost control. The problem in a larger organization (and there are over 800 engineers on site in Edinburgh) is ensuring that the cost drivers and potential trades are known about by all project team members and, in particular, enabling those team members, with little or no domain experience, to play their role. Part of the solution has been to establish a top down review of the controllable product cost on a regular basis. This short, sharp meeting requiring answers to: cost now; cost future with dated action plans; and relevant design margin analysis or shop floor data (depending on lifecycle stage).

6. CONCLUSION

An effective laser design and manufacturing capability has been developed by SELEX Galileo. While the starting point was the knowledge developed in the early years of the laser, this has been built on and enhanced successfully through continued innovation and attention to detail over the last 8 years. Over 1200 lasers have been built and shipped since 2005.

7. ACKNOWLEDGEMENTS

REFERENCES

[1]   [Ferranti: 50 Years in Scotland], GEC Marconi Avionics Ltd, Edinburgh, 26 (1993).
[2]   The Association of Industrial Laser Users, Awards 2001.
      www.ailu.org.uk/association/awards_and_prizes/ailu_awards/award/2001_david_dyson.html
[3]   Muir, A., private communication, (2010).
[4]   Ward, R. D., "Improvements Relating to Lasers," GB 1358023 (A) (1972)
[5]   Heywood, P. J., Eggleston, R. A., "Optical Modulators," GB2209609 (B) (1987)
[6]   G. Gould, S. Jacobs, P. Rabinowitz, and T. Shultz, "Crossed Roof Prism Interferometer," Applied Optics, 1, 533-534 (1962).

[7] M. K. Chun and E. A. Teppo, **"**Laser resonator: an electrooptically Q-switched Porro prism device," Applied Optics, 15, 1942-1946 (1976).

[8] Ajer, H., Landrø, S., and Stenersen, K., "Numerical Simultations of Diode Side-Pumped Q-Switched Nd:YAG Laser Oscillators and Amplifiers with Rod and Zig-Zag Slab Crystal Geometry," OSA proceedings on Advanced Solid State Lasers, 20, 20-24 (1994).

[9] Hestenes, D, [New Foundations for Classical Mechanics], Kluwer Academic Publishers, Dordrect/Boston/London, 1-104 (2003).

[10] Hanlon, J., Ziock, H., "Using Geometric Algebra to understand pattern rotations in multiple mirror optical systems," Report Number LA-UR--97-721, Los Alamos National Lab., NM (United States). http://www.osti.gov/bridge/product.biblio.jsp?osti_id=468622

[11] Spencer, G. H., Murty, M. V. R. K., "General Ray Tracing Procedure," J. Opt. Soc Am. **52**, 672-678 (1962).

[12] Schweitzer, N., Friedman, Y., Skop, M., "Stability of systems of plane reflecting surfaces," Applied Optics, 37, 5190-5192 (1998).

[13] Nilsson, A. C., Gustafson, E. K., Byer, R. L. "Eigenpolarisation Theory of Monolithic Non Planar Ring Oscillators," IEEE J. of Quantum Electronics **25**, 767 (1989).

[14] Smith, A. V., Armstrong, D. J., "Nanosecond optical parametric oscillator with 90˚ image rotation: design and performance," J. Opt. Soc. Am B, **19**, 1801 (2002).

[15] Barr, J. R. M., Legge, D., MacLean, J. R., Thorne, D., Truby, J., "Optical Parametric oscillators," EP2007/064033 (2007).

[16] White, A., Hall, G., Barr, J., McElhinney, M., Thiagarajan, P., Cao, C., "Thermally insensitive laser diode arrays," Proc. SPIE 7325, 73250P (2009).

[17] Barr, J., White, A., Moore, S., "Laser Apparatus and method of operation," WO/2012/069409, (2012).

[18] Canham, J. S., "Revisiting mechanisms of molecular contamination induced laser optic damage," Proc SPIE 67200M-11 (2008).

[19] Hovis, F. E., Shepherd, B., Radcliffe, C., Maliborski, H., "Mechanisms of Contamination Induced Optical Damage in Lasers," Proc SPIE 2428, 72 -83 (1995).

[20] Hovis, F. E., Shepherd, B. A., Radcliffe, C. T., Maliborski, H. A., "Contamination damage in pulsed 1μm lasers," Proc SPIE 2714, 707-715 (1996).

[21] Belford Research, www.belford-research.co.uk.

[22] Becker, S., Pereira, A., Bouchut, P., Geffraye, F., Anglade, C., "Laser-Induced Contamination of Silica Coatings in Vacuum," Proc SPIE 6403, 64030J-1 – 64030J-12 (2007).

[23] Sharps, J. A., "Reliability of hermetically packaged 980nm diode lasers," LEOS '94 Annual Meeting, Conference Proceedings, 2, 35 (1994).